Journal of Coastal Research	16	2	316–328	Royal Palm Beach, Florida	Spring 2000

Sediment Dynamics in the Lowermost Amazon

Helenice Vital† and Karl Stattegger

Geologisch-Paläontologisches Institut und Museum der Christian-Albrechts-Universität
Olshausenstrasse 40
24118 Kiel, Germany
e-mail: helenice@geologia.ufrn.br

ABSTRACT

VITAL, H. and STATTEGGER, K., 2000. Sediment dynamics in the lowermost Amazon. *Journal of Coastal Research,* 16(2), 316–328. Royal Palm Beach (Florida), ISSN 0749-0208.

The sedimentological character of material in transport and on the riverbed were investigated in order to record the sedimentary dynamics in the lowermost Amazon. Suspended sediment concentration measurements show that net deposition occurs on the delta plain (between Obidos and the Xingu River), while downstream suspended sediment transport remains approximately constant. Lateral sediment input is compensated by erosion in deeply incised channels keeping the region in a dynamic equilibrium. The surficial distribution of bedload sediments carried by the Amazon shows a corridor of sands (channel deposits) bordered by silty sediments at the margins. It consists chiefly of very fine sands, which become fine and medium-coarse sands laterally (Figure 6). The development of bedforms on the sand surface reflects strong bottom currents and sediment transport, as well as tidal effects. Nearshore sedimentary facies identified were interlaminated fine and coarse silt, interlaminated silt and sand, faintly laminated mud, and mottled mud.

ADDITIONAL INDEX WORDS: *River-ocean interactions, sedimentation processes, sediment mapping, grain size, stream incision, Amazon River.*

INTRODUCTION

The Amazon system encompasses an immense and complex area, diverse in both climate and rock types, that extends from the Andes to the Atlantic Ocean. The river supplies over a trillion cubic meters of water, a billion tons of sediment, and nearly a billion tons of dissolved solids to the Atlantic Ocean annually. The annual flow of the Amazon River alone is estimated to be almost 20 percent of the total annual runoff from all land areas (GIBBS, 1967; OLTMAN, 1968). Comparable sediment load of that order of magnitude is known only from the Ganges-Brahmaputra and the Yellow River systems (KUEHL *et al.,* 1997). At the river mouth the Amazon discharge interacts with vigorous wind-driven, buoyancy and tidal currents, and semi-diurnal tides with ranges of more than 3 meters. Semi-diurnal tides with smaller amplitudes are also observed 800 km upstream near Obidos. These features plus the river's nearly natural state make the Amazon a fascinating place and unique natural laboratory to study a number of important processes in sedimentology.

Numerous studies have dealt with the sedimentology and dynamics of the upper Amazon, as well as of the Amazon continental margin (*e.g.* MILLIMAN *et al.,* 1975; NORDIN *et al.,* 1980; FRANZINELLI and POTTER, 1983; MEADE *et al.,* 1985; IRION and ZÖLLMER, 1990; NITTROUER and KUEHL, 1995; NITTROUER and DEMASTER, 1996). On the other hand, almost no attention has been devoted to the zone between them, a distance of 800 km, from the town of Obidos to the ocean (Figure 1). However, it can be assumed that this transition region is important in understanding the sediment dynamics of the overall system. For example, existing data indicate that a large fraction of Amazon discharge (about a third) could be trapped in its delta plain and mouth (MEADE, 1994; NITTROUER *et al.,* 1995).

The aims of this study were to observe for the first time the sediment dynamics and to record the sedimentological character in this hitherto unknown portion of the Amazon River. Moreover, the results which were obtained provide a better understanding of the sedimentary processes interacting in a large river-estuary/subaqueous delta-ocean system. Studies were carried out from the Xingu river mouth upstream to the town of Macapa downstream, including the Estreitos, a channel net-work which link the Amazon and Para rivers (Figure 1).

VITAL (1996) and VITAL *et al.* (1998) subdivide the lowermost Amazon into five areas based on the riverbed morphology observed by high-resolution bathymetric, shallow seismic reflection and side-scan sonar analysis: Xingu Mouth (XM), Amazon North Branch (ANB), Amazon South Branch (ASB), Estreitos (EST) and Jari Mouth (JM). The division of the lowermost Amazon in these five areas are also used in this study (Figure 1).

Results of detailed studies on mineral composition and provenance are presented in another paper (VITAL *et al.,* 1999).

METHODS

Fieldwork was conducted during different seasons of river discharge (peak, in June–July 1991; low, October 1991 and

96128 received 12 October 1996; accepted in revision 15 May 1999.

† Present Address: Dept. Geologia-CCET/PPGG, Universidade Federal do Rio Grande do Norte, Campus Universitario, Natal-RN, 59072-970, Brazil.

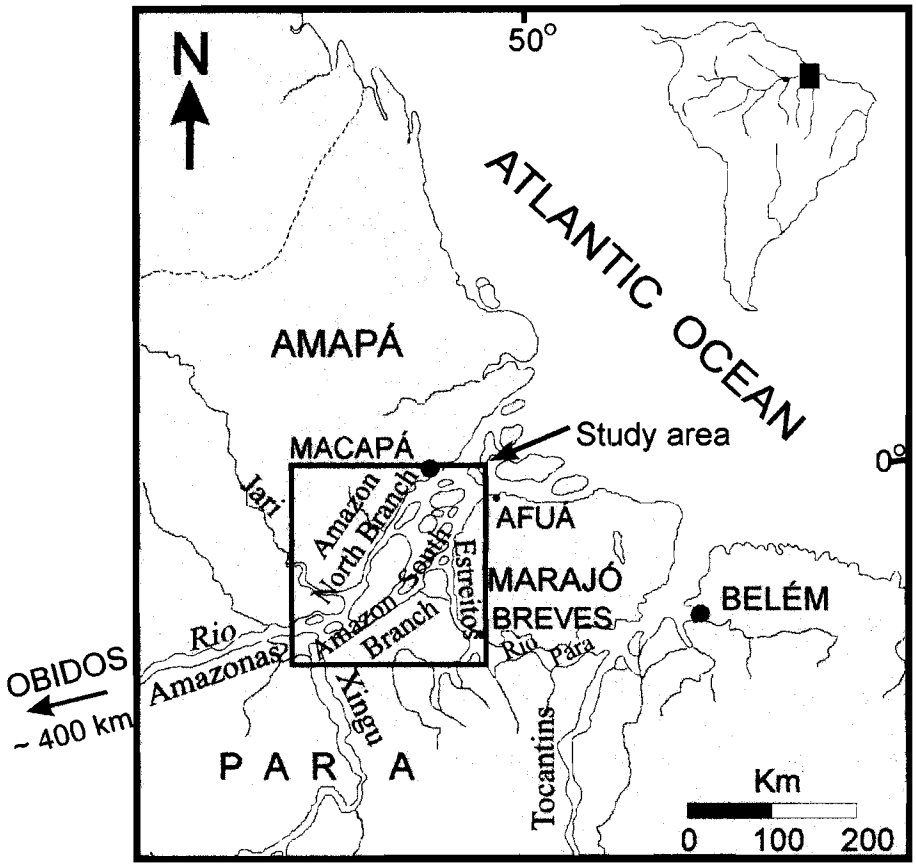

Figure 1. Location of the study area.

November–December 1994; rising, January–February 1994), using the small research boat CURUPIRA from Federal University of Para-Brazil. Sediment samples were collected in channels by dredge and bottom-grab ("van Veen"). At the river margins vibracores and pushcores up to 4 m in length (7.5 cm diameter aluminum barrels) were obtained.

Suspended sediment samples were collected just below of the water surface and at 5 m depth, during low and rising discharge, with a Niskin bottle sampler. Sediment concentrations were determined by the weight of sediment collected on a tared Millipore filter (with nominal pore size of 0.00045 mm). At the same time the conductivity, salinity and temperature of the water were measured with a Yellow Springs sensors (YSI, model 57 and model 33). Additionally, during low discharge (1991), suspended sediment profiles were obtained with a CTD/Datalogger (Ocean Sensors, model OS100), an OBS (Optical Backscatterance Sensor, made by D & A Instruments) and a rotor current meter (Marsh-McBirney, model S12 electromagnetic current meter). Sediment concentrations were determined by converting output from an OBS using calibration based on *in situ* pump samples. These sensors are capable of measuring particles concentrations from 5 $mg \cdot l^{-1}$ up to 300 $g \cdot l^{-1}$.

Cores were sectioned lengthwise in the laboratory with a circular saw, then photographed, described, X-rayed, and sub-sampled for grain size and mineralogy. Grain-size measurements for the mud fraction were made using a SediGraph model 5100 automatic particle-size analyzer and for the sand fraction by dry sieving at ½ Phi interval. Determination of carbonate (decomposition with H_3PO_4) and total organic carbon (combustion) was performed by a Coulomat 702. From the C_{total} and C_{CO_2} values, the C_{org} content was calculated by subtraction.

RESULTS AND DISCUSSION

Suspended Sediments

Of the three major transport loads carried by rivers—*bedload, suspended,* and *dissolved*—suspended sediment is by far the largest. Computations have estimated that in the lower Amazon, bedload discharge makes up only one percent of the suspended-sediment discharge as a whole (MEADE, 1988).

The seasonal variations in water discharge (Q), current velocity (CV) and suspended sediment concentrations (SSC) measured at Obidos, Altamira and Sao Francisco gauge stations are shown in Figure 2. Obidos is located 800 km from the Atlantic Ocean and is the first town upstream the Amazon River where the tidal range is <1 m; Altamira is located on the Xingu River 700 km from the Atlantic Ocean and 200 km from the mouth of the Xingu; Sao Francisco is located on

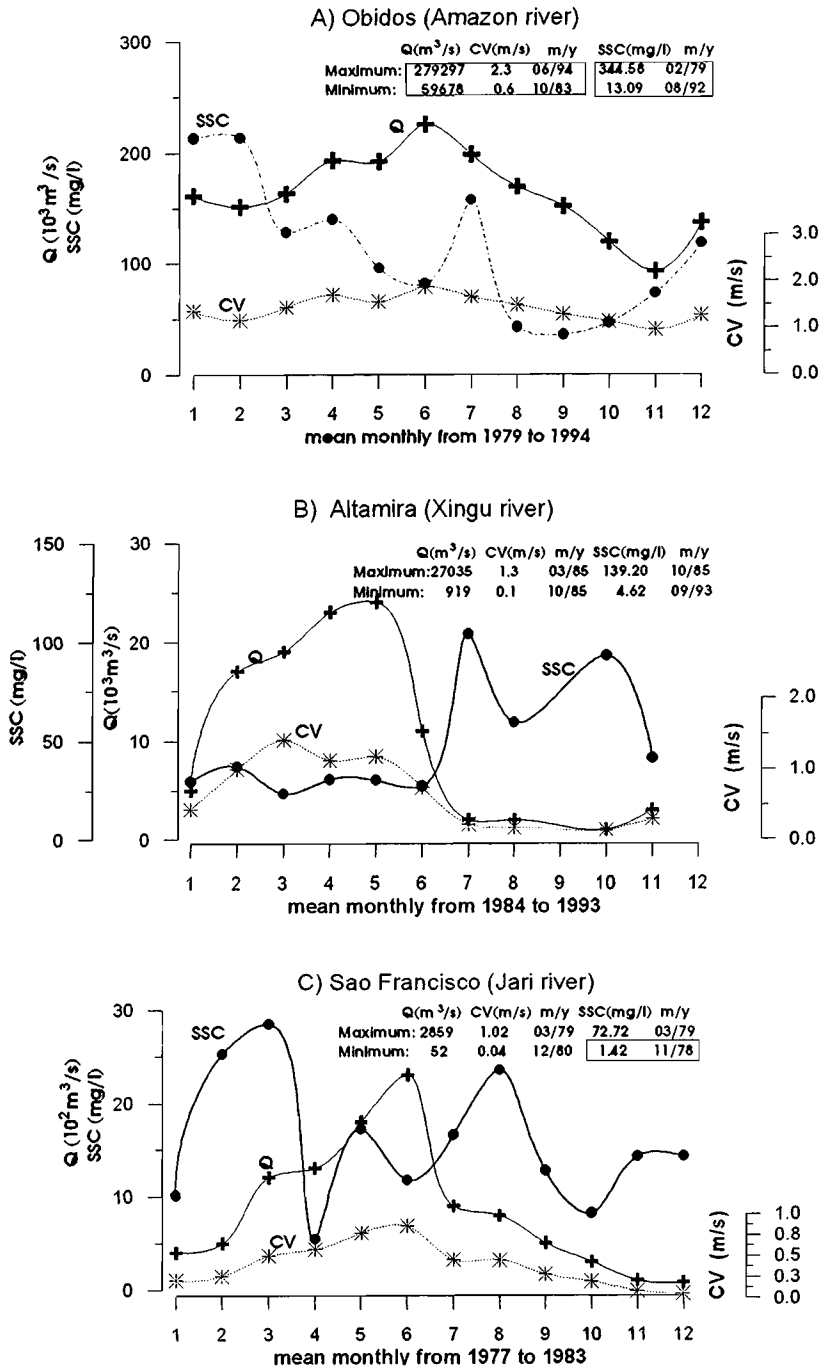

Figure 2. Variations in water discharge (Q), current velocity (CV) and suspended sediment concentrations (SSC) measured on A) Obidos, B) Altamira and C) Sao Francisco gauge stations. Data provided by the Brazilian agency DNAEE/MME.

the Jari River 530 km from the Atlantic Ocean and 100 km from the mouth of the Jari.

The maximum water discharge in the lowermost Amazon occurs between April and July and the minimum between October and December, with the sediment concentration peak coinciding with the rising water discharge and the minimum sediment concentration with the falling water discharge (Figure 2a). The difference between high and low water discharge is only a factor of about 2–4, because the large drainage basin straddles the equator and has segments that flood at different times during the year (MEADE *et al.*, 1991). On other hand, the Xingu and the Jari, both tributaries of the Amazon, show abrupt differences between high and low waters with a factor of about 30 for the Xingu and about 50 for the Jari

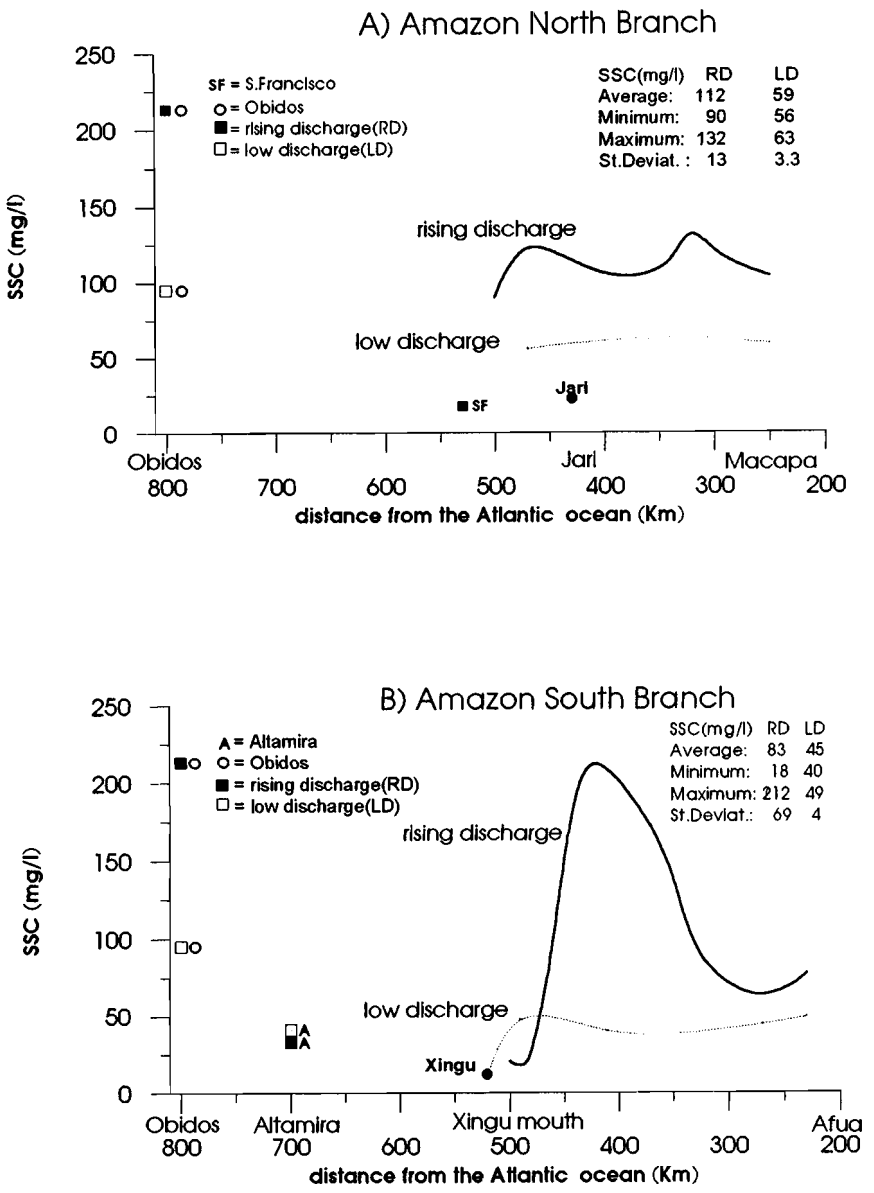

Figure 3. Patterns of seasonal variability of suspended sediments concentration (SSC) at surface water from a 300 km reach of the lowermost Amazon. 3A) Amazon North Branch; 3B) Amazon South Branch. Data from Obidos (O), Altamira (A) and Sao Francisco (SF) gauge stations provided by the Brazilian agency DNAEE/MME.

(Figure 2b, c); the suspended sediment concentration (SSC) is insignificantly low when compared with the white waters of the Amazon as both the Xingu and the Jari are clear water rivers. The Xingu has SSC peaks coinciding with its low water discharge, and the Jari has various SSC peaks throughout its seasonal cycle, probably reflecting another pattern of seasonal storage and resuspension. The current velocity is closely correlated with the water discharge at all three gauge stations.

Figure 3 shows two profiles, the Amazon North Branch (Figure 3a) and the Amazon South Branch (Figure 3b), sampled at water surface during rising and low water discharge. During low discharge the SSC (dashed line) was uniform in both the Amazon North and South Branches with a minimum of 40 mg/l, a maximum of 63 mg/l and a standard deviation of about 3 mg/l. The smallest value refers to the Xingu river waters with only 10 mg/l but rises suddenly when they mixed with the Amazon waters. The SSC increases during high discharge (thick line) reaching more than 200 mg/l. The Amazon South Branch shows strong variability (Standard deviation about 70 mg/l), although the average (83 mg/l) is much smaller than in the Amazon North Branch which shows an average of 112 mg/l and a Standard Deviation of 13 mg/l. The smallest value was obtained in the Jari River and at the mouth of the

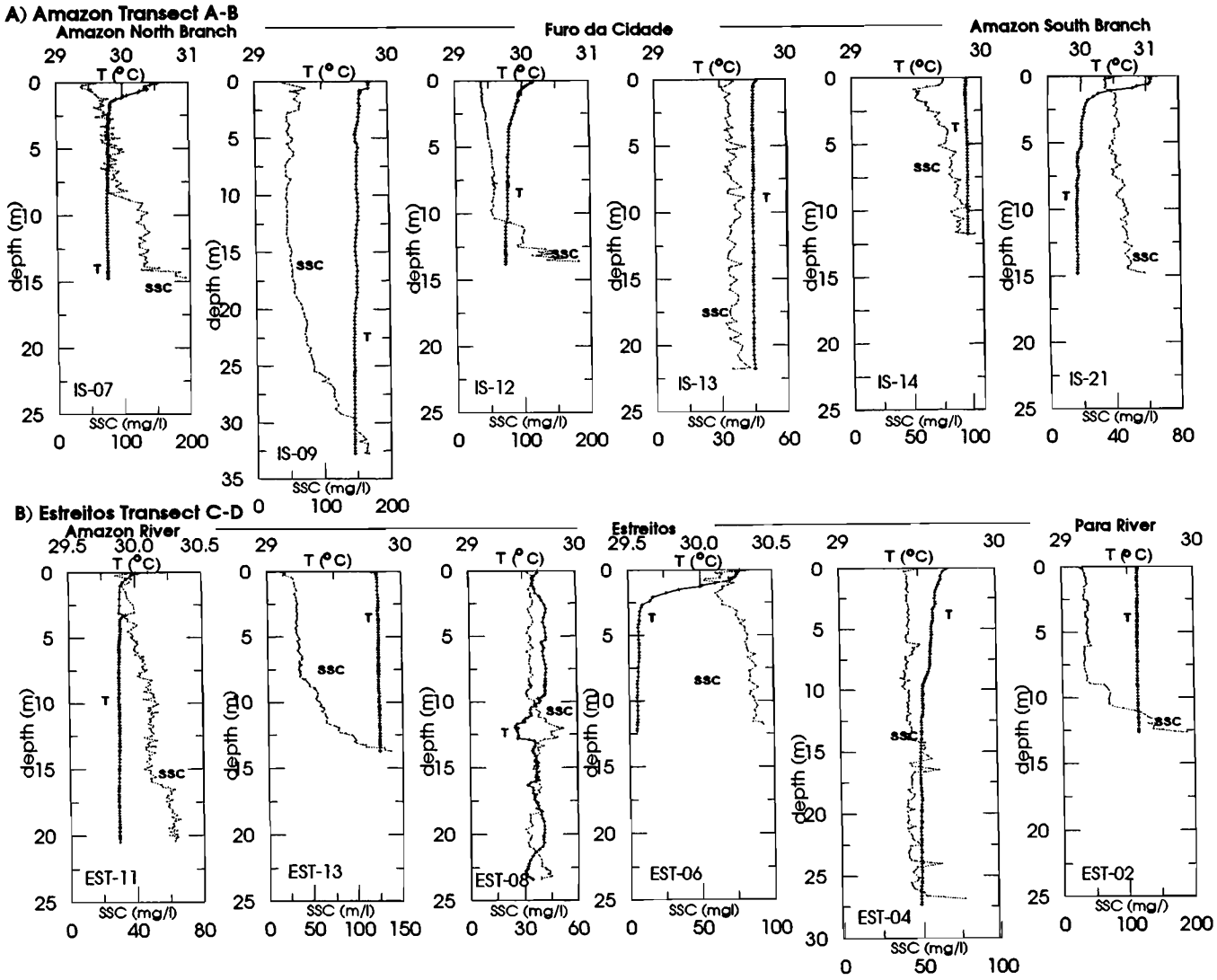

Figure 4. The behavior of suspended sediment concentrations (SSC) and temperature (T) in the water column is shown by profiles obtained by the suspended-sediment profiler. The profiles are divided into two transects: A) Amazon transect A–B, from Amazon North Branch to the Amazon South Branch through Furo da Cidade, and B) Estreitos transect C–D, from Amazon to Para river through the Estreitos. Data collected during low discharge. For location (A, B, C, D) see Figure 6A.

Xingu with 23 and 18 mg/l respectively. This data shows that suspended sediment transport remains approximately constant within the study area, and the fact that there is little surficial sedimentation through lateral sediment input keeps this region in a dynamic equilibrium. The same pattern can be observed downstream in the North and South Channels (TORRES & STATTEGGER, 1995). However, when these data are compared with those measured upstream, they fit in well with the Altamira and the Sao Francisco gauges but not with that of Obidos (Figure 2a,b,c). The suspended sediment concentration decreases about 40–50% from Obidos to the lowermost Amazon, suggesting that net deposition is occurring mainly on the delta plain of the Amazon (between Obidos and the Xingu River). Irregular peaks observed at rising discharge probably reflect the influence of strong currents (in excess of 2 m s^{-1}) as well as the tidal action, which together promote the extensive erosion of the channel margins and resuspension of the riverbed sediments, thus increasing the SSC.

Suspended sediment concentration profiles taken during low discharge in the Amazon and in the Estreitos were homogeneous throughout most of the water column, increasing slightly to the bottom. The water properties of salinity (zero) and temperature (29–31°C) also were homogeneous, indicating a well-mixed water column. Two transects are shown in Figure 4: (1) Amazon (A–B), from the Amazon North Branch to the South Branch, through Furo da Cidade, and (2) Estreitos (C–D), from the Amazon to the Para River, through the Estreitos.

In the Amazon transect A–B (Figure 4a), the SSC at the

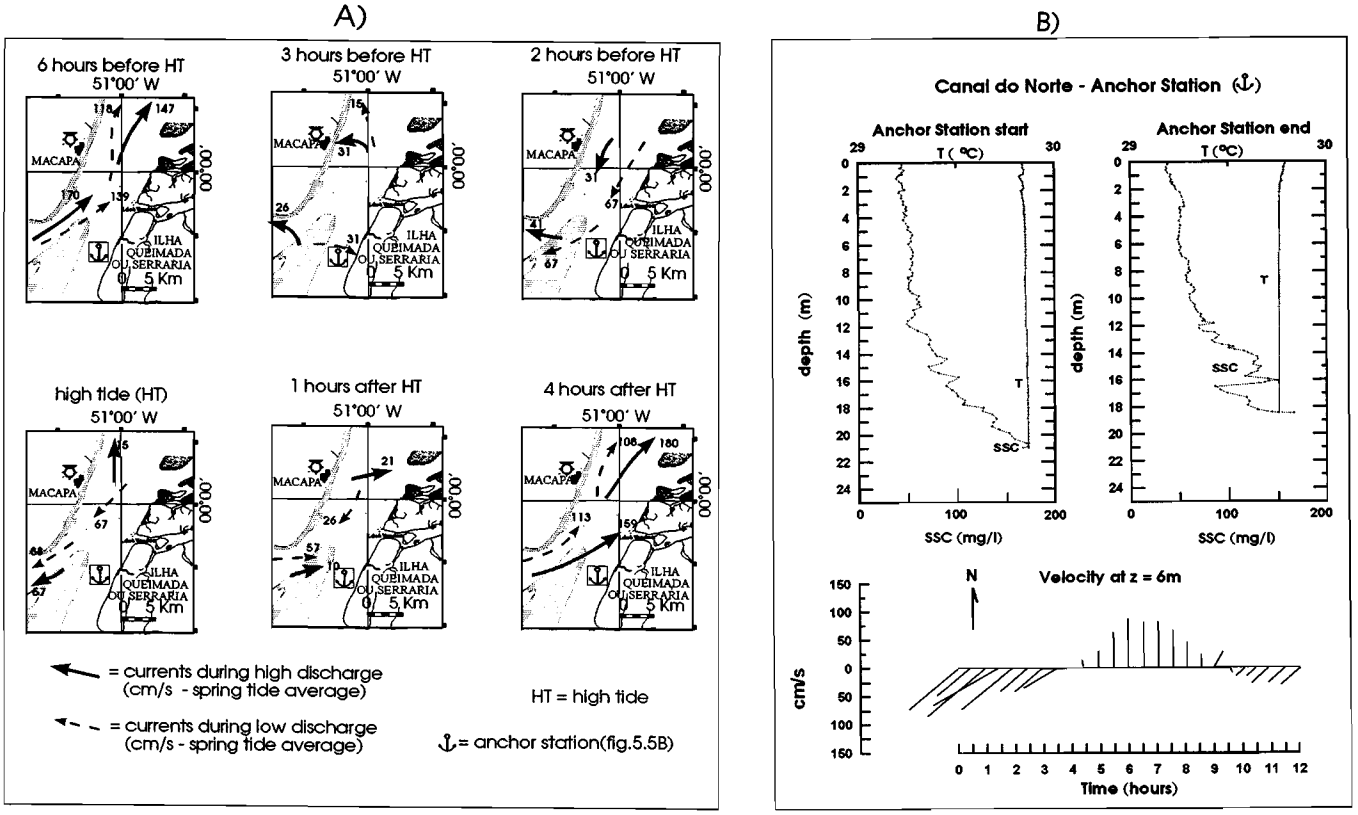

Figure 5. Currents variations between high and low discharge (A) and a low-discharge time series for anchor station located at ANB (B). A) shows the current circulation at different times in relation to high tide (modified from DHN Amazon currents chart, 1981); B) shows two suspended sediment concentration profiles (SSC) and a velocity time series of position z = 6 m above river bed. Tidal range in this area = 4 m.

bottom is generally 2 to 5 times more than at the water surface, with the smallest values toward the Amazon South Branch. These values differ from GIBBS (1967) and CURTIS *et al.* (1979). Gibbs reports that the SSCs at the water's surface is about half the average at the bottom, and CURTIS *et al.* maintains that samples collected at 0.9 total depth in the Amazon had only a 20% greater SSC than samples collected from river surface. The differences are probably related to differences in the sampling procedures.

In the Estreitos transect C–D (Figure 4b) the SSCs at the bottom are on the average 3–5 times greater than at the water's surface and some places can reach peaks at the bottom of the water column as high as 200 mg/l. Since salinity and temperature remained invariable, high-concentration suspensions are interpreted as the result of erosion and resuspension from the bottom and from the margins, principally because of the narrowness of the channel.

To address tidal variability in the Amazon an anchor station consisting of half-hourly casts with a current meter was set up for 12 hours in the Amazon North Branch in front of the city of Macapa. Suspended sediment profiles were taken at the beginning and end of the measurements (Figure 5). The tides behave as a progressive wave that propagates into the mouth of the river and reaches as far as Obidos (BEARDSLEY *et al.*, 1995). The variations of the tidal currents in this area between high and low discharge are presented in Figure 5a and the typically semidiurnal tidal flow is shown by a stick diagram (Figure 5b). The SSC profiles do not show any differences, both ranging from 50 mg/l at the water surface to about 170 mg/l at the bottom (Figure 5b).

Bottom Sediments

Grain Size

The spatial distributions of different grain size classes in the lowermost Amazon have been mapped. Figure 6 reveals significant trends in the sand and silt fractions. Grain-size distribution are based on samples from the riverbed and on interpretations from the seismic profiles (VITAL, 1996; VITAL *et al.*, 1998). A corridor of sand bordered by silty sediments at the margins can be observed throughout the area, clearly reflecting the intensity of the hydraulic regime in which the grains were transported and deposited. Deposition of silt (and minor amounts of clay) can be observed at the mouth of several tributaries entering the Amazon (*e.g.* Xingu, Jari). Old river substrate (overconsolidated deposits) is exposed downstream near Macapa and Afua.

In the Amazon the "corridor of sand" is predominantly very fine sand, that can vary laterally to fine and only rarely to medium-coarse sand. Generally, grain size tends to decrease

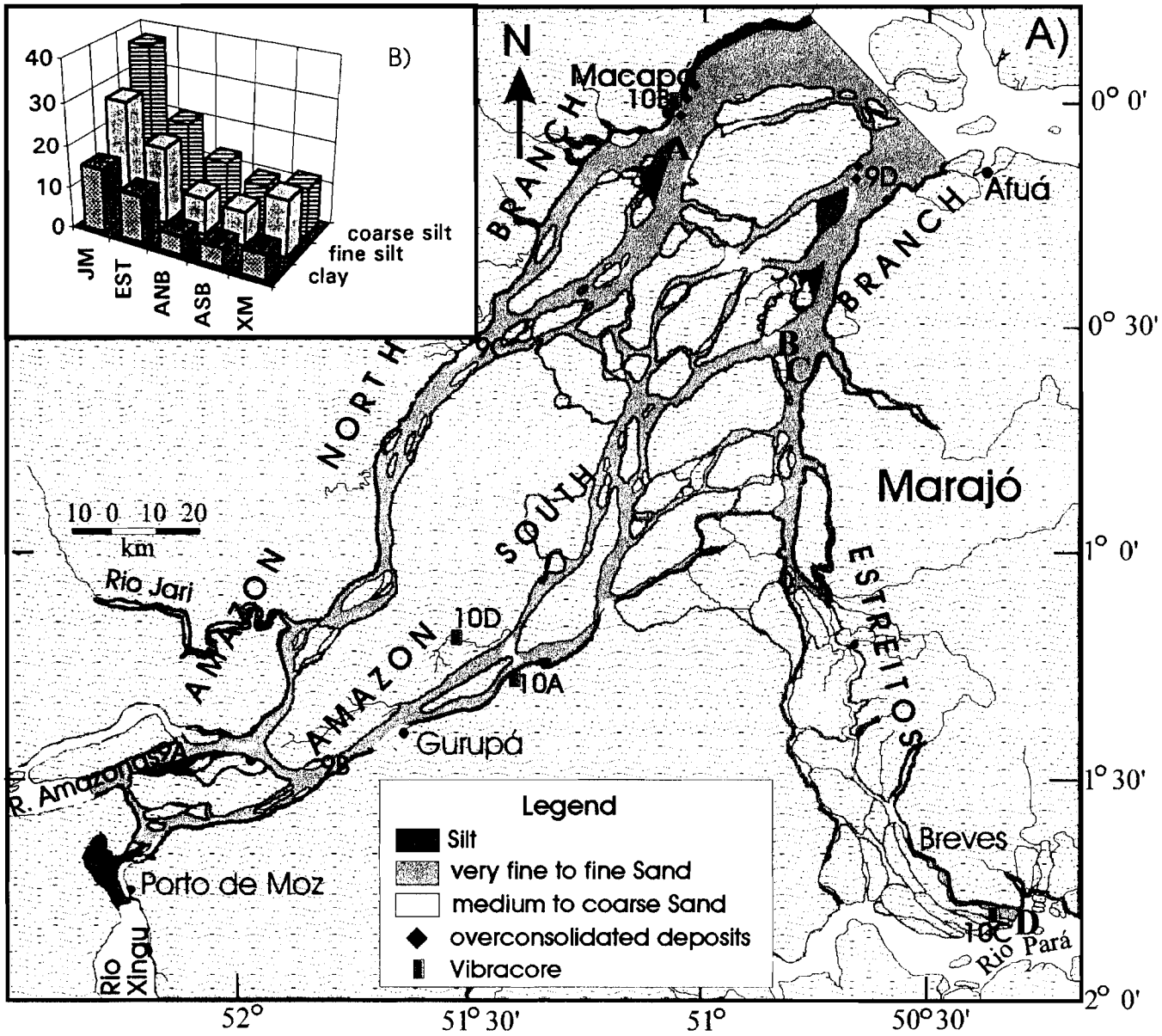

Figure 6. A) Grain-size distribution map. B) Histograms of mud-fraction distributions. ANB = Amazon North Branch (n = 37), ASB = Amazon South Branch (n = 43), EST = Estreitos (n = 26), XM = Xingu Mouth (n = 7), JM = Jari Mouth (n = 6). n = number of samples. Coarse silt fraction = 0.063–0.016 mm, fine silt fraction = 0.016–0.002 mm, clay fraction = <0.002 mm. A, B, C and D refer to the transects displayed in Figure 4. 9A, 9B, 9C and 9D refer to the location of the bedform types displayed in Figure 9. 10A, 10B, 10C and 10D refer to the location of the core profiles displayed in Figure 10.

from the scour, where the coarsest size is found, to the channel margin, where fine particles are deposited as water velocity decreases and the flow stagnates, although there is no significant change in texture downstream. In the Estreitos, the corridor of sands changes from very fine sand at its extremities (close to the Amazon and the Para Rivers) to fine, and medium sand in the central part. Differences in texture from silty sediments bordering the sands are also observed: while in the Amazon they are mostly coarse silt, in the Estreitos they are essentially fine silt (see also section on sedimentary structures).

The histograms displayed in Figure 6b show the means for the fine-grained fraction (<0.063 mm). JM has the highest amounts of the clay fraction and the smallest of sand; XM, in spite of being characterized by silty sediments at the channel, shows a dilution effect because of the presence of sands which are matrix-free at the margins; XM, ANB and ASB have the greatest amounts of sand. EST is in an intermediary position, reflecting the fine fraction from the margins and the relatively coarse fraction from the channel. Gravel fraction is scarce, occurring only in sediments from the main scour or as rip-up-clasts, which are gravel composed of pebbles from

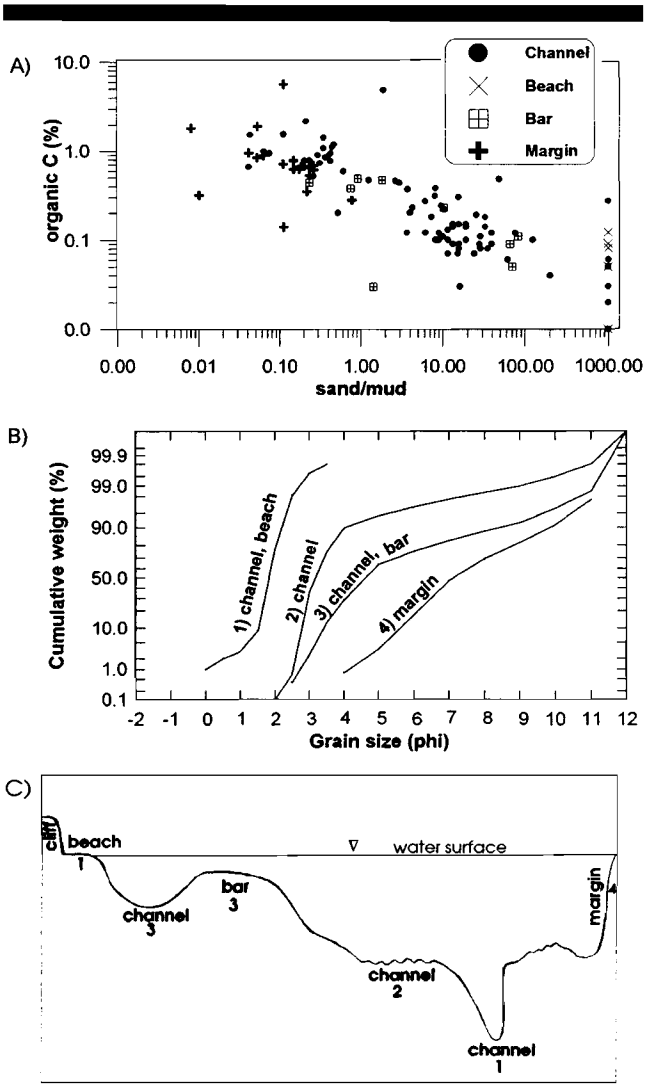

Figure 7. A) Organic C and clastic ratio (sand/mud) relations. B) Classes of cumulative curves related to different deposits. C) An idealized sedimentological cross section.

subrecent (?) and recent consolidated mud sediments. They are of local origin, and are not found at a great distance from the place of their formation. Therefore, they develop mainly in channels, by the erosion of their walls, or within the reach of high tide currents by the erosion of subrecent consolidated silty clay (downstream near Macapa and Afua). The mean grain size of these mud pebbles falls almost invariably into the silt fraction, which generally accounts for more than 70% of the total fraction.

Organic carbon contents of sediment samples are also related to the grain size. With a range from 0 to 6% they are inversely correlated to the sand:mud ratio (Figure 7a). This reflects the similarity in the settling velocity, *i.e.* hydrodynamic or hydraulic equivalence, of the organic constituents and of the fine-grained mineral particles (TRASK, 1939), and/or it reflects the greater surface area of finer particles (sediment specific surface area) and the amount of organic carbon that may be adsorbed on their surfaces (TYSON, 1995).

The analysis of grain size data was based on the concept of the *sample suite:* a set of closely related samples taken from a single transport and/or depositional system (TANNER, 1991, 1995). This kind of analysis has the advantage of avoiding the great number of plotted points which clutter the diagrams with dubious or anomalous points, thus facilitating the differentiation between the effects of various transport agencies as well as the identification of the transitions from one agency to another.

In this way, the analysis of the characteristics of the grain size data provided four well-defined classes of cumulative curves (Figure 7b), each related to a different group of size, that in turn are related to different deposits (Figure 7c): 1) channel and beaches sediments, fine to coarse sand (traction population, strong currents); 2) channel, very fine to fine sand (mostly traction population, minor amounts from saltation and suspension); 3) channel and bars, silt to very fine sand (saltation and suspension population); and 4) margin, essentially silt deposited from the suspension population (weak currents).

Grain size parameters are valuable in discriminating depositional subenvironments (Figure 8). Mean and sorting reflect the flow strength and the degree of uniformity in the deposit produced by current action during grain transport and deposition (Fig. 8a). The margin sediments are very poorly sorted and strongly fine skewed, while beach sediments are moderately to well-sorted and negatively skewed (coarse-tailed). Bar sediments are poorly sorted and strongly fine skewed. Channel sediments are poorly sorted and fine skewed overlapping with bar, and more rarely, with beach sediments (Fig. 8b). A slight increase in sorting could be observed in Estreitos from its extremities to the center (from moderately to well-sorted).

Sedimentary Structures

The range, size and character of alluvial bedforms are direct products of the contemporary balance between erosion and deposition at different points on the bed, and sediment size is probably the most important determinant of their development (REID and FROSTICK, 1994). Four sedimentary facies are identified in the sediment of the Amazon margins, based on characteristic sedimentary structures observed in radiographs of sediment cores. In addition, the "corridor of sands" (channel deposits) was characterized by visual observations of grab samples and bedforms examined by seismic reflection profiles (VITAL, 1996; VITAL *et al.*, 1998). The nature and spatial relationships of these facies are described below.

The sandy layer, which covers the channel deposits throughout the area, is chiefly composed of very fine sands that change laterally to fine and medium-coarse sands. Asymmetrical and symmetrical sandwaves are common, indicating high bottom currents and sediment transport as well as tidal effects (Figure 9). Where bars emerge at low tide, forming small islands, ripples are observed on the sandy surface. Visual observations from grab samples include lamina-

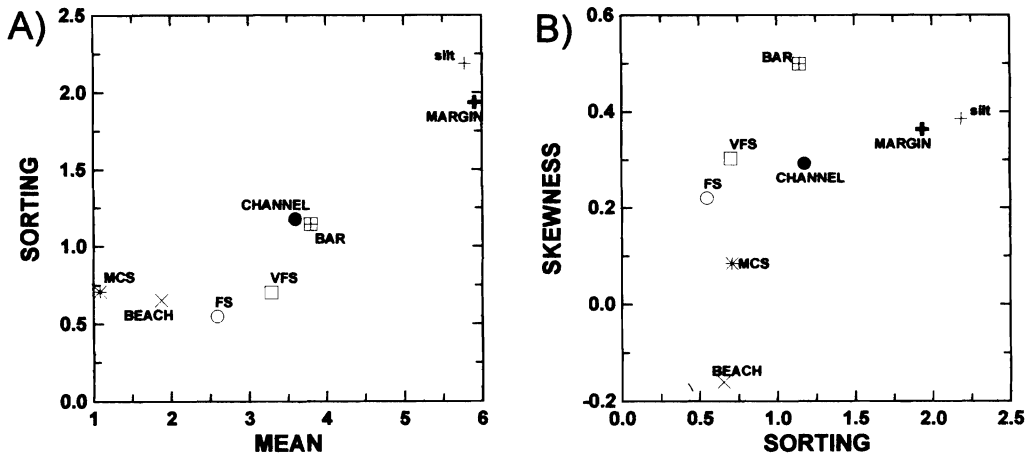

Figure 8. Scatter plots of "sample suites" based on the grain size parameters mean, sorting, and skewness. VFS = very fine sand (n = 23), FS = fine sand (n = 34), MCS = medium to coarse sand (n = 10), silt (n = 50). n = number of samples. A) mean vs. sorting; B) sorting vs. skewness.

tions and rip-up clasts. The rip-up-clasts became very abundant downstream, where the symmetrical sandwaves dominate and demonstrate that the strength of the currents is sufficient to erode consolidated mud deposits. This facies probably correspond to the physically stratified sands defined by KUEHL *et al.* (1986) in the Amazon subaqueous delta, which probably continue landwards in the riverine part of the Amazon mouth, and the same nomenclature has been used in this study. It is also equivalent to the clean sands in the North and South channels of the Amazon defined by TORRES and STATTEGGER (1995).

The four sedimentary facies identified from the marginal deposits are *interlaminated fine and coarse silt* (1), *interlaminated silt and sand* (2), *Faintly laminated mud* (3), and *mottled mud* (4). Typical examples are documented in Figure 10.

Interlaminated Fine and Coarse Silt. This facies extends along the Amazon North and South Branches (ANB, ASB), from the upstream limit of the studied area until the downstream end of Gurupa Grande Island. It is characterized by 10–20 cm thick beds of laminated fine and coarse silt with a thickness of about 1 mm. The contact between laminae is rather sharp. This suggests that lamina formation is usually associated with conditions of increased bottom shear stress and consequent erosion of the riverbed (KUEHL *et al.*, 1988); according to these authors, the silt particles that form the laminae are probably supplied both from sorting processes operating on the riverbed (*e.g.* bedload sorting, winnowing of fines) as well as from changes in the nature of sediment supplied from suspension. Discrete massive beds (about 10 cm thick) of very fine sands occur sporadically and may represent more energetic floodplain traction currents, such as those that deposit crevasse splays. Old roots cast throughout and ripple cross-lamination can also be observed. Generally, the upper 20–30 cm contains more clay and burrows are frequent. Near XM this upper clay layer is replaced by very fine sand.

Interlaminated Silt and Sand. Downstream, as a continuation of the foregoing facies (or transition between the delta plain and the river mouth), faint coarse silt laminations alternate with faint very fine sand laminations. The intermediate grain size, between the coarser and finer end members, suggests traction-plus-fallout deposition. According to Ricci-Lucchi (1995) these structures are common in deposits of fluvial floods. Because of the Amazon's high water discharge throughout the year, which is associated with its strong currents (in excess of 2 m/s), and because of its high tidal range in this area (about 4m), the Amazon's semi-diurnal fluctuations behave as a true daily flood, and could thus explain the traction-plus-fallout deposition. Cross-laminations, old burrows and partially decomposed wood fragments are frequent, as well as more sporadically visible mica flocs. This facies is related to fine-grained beaches exposed during low tide. The formation of mud pebbles along these beaches is common. A vibracore from this area (VC-12, taken in front of Macapa City) reached the bed substrate. A strong contact between this substrate and Amazon sediments can be observed at 326 cm and is characterized by a red lateritic weathering horizon, composed of hematite granules and pebbles. The lateritic weathering is followed by alternating beds (2–10 cm) of laminated kaolinite clays and faint laminated coarse sand (essentially quartz). Differential loading structures can occur at clay/sand interlayers, where broader downbulges of sand sink into the clay, defining load casts. This substrate is related to the Barreiras Formation and to the seismic horizon "B" from VITAL (1996) and VITAL *et al.* (1998).

Faintly Laminated Mud. This facies is characteristic of the Estreitos area. Thin (<1 mm) coarse-silt laminae alternate with very faintly laminated mud (1–5 cm) composed of fine silt and clay. The sand fraction, with rare exceptions, is less than 5% or even zero. At the top, laminations are commonly obscured by root development. Wood fragments and organic layers (partially decomposed material) can frequently be observed. Both, oyster shell debris and a basal peat layer were found in a pushcore from this area. Peat accumulations are not common in most tropical rain forests because the organic matter rapidly deteriorates on the floor. The main feature of

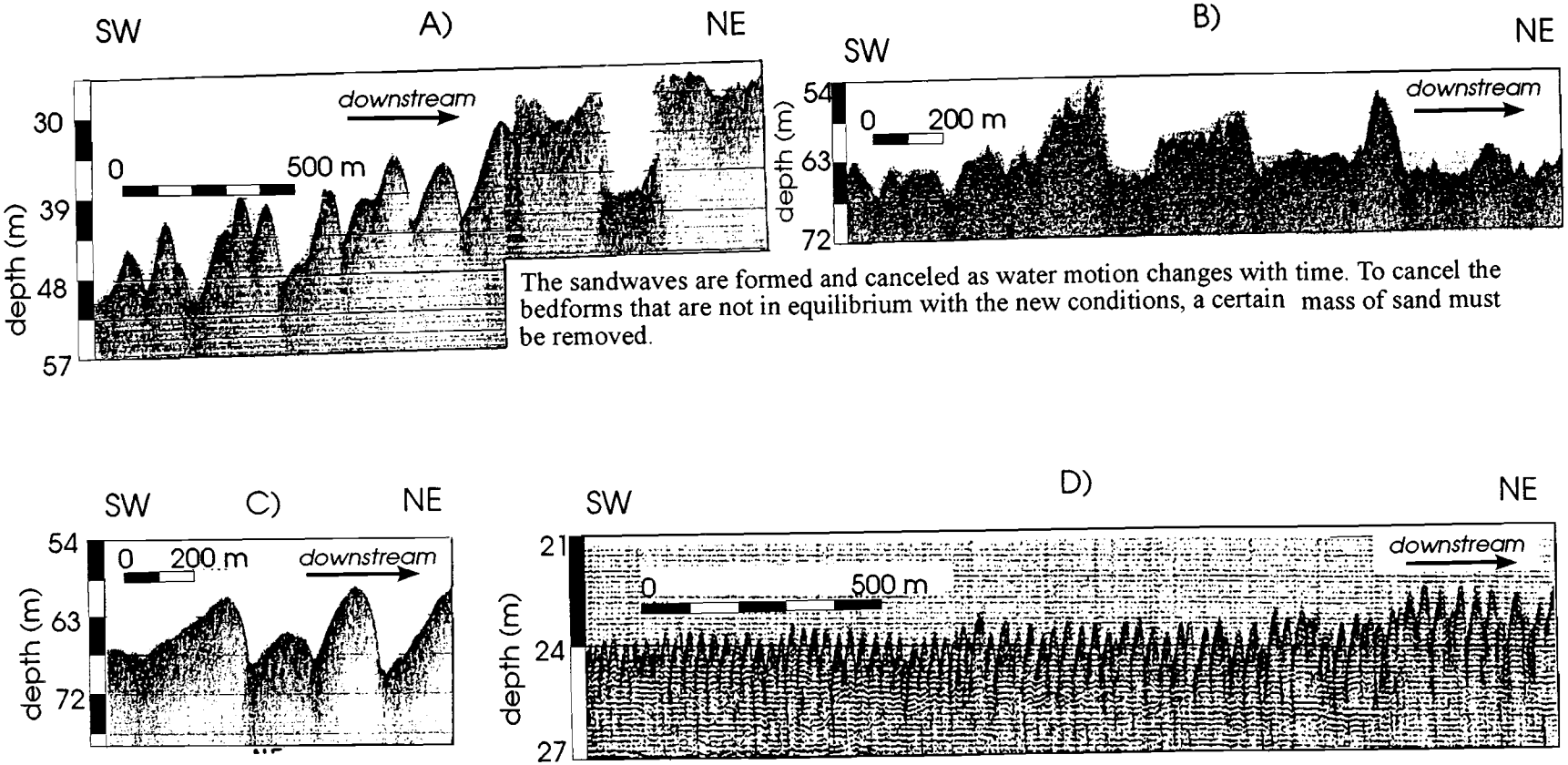

The sandwaves are formed and canceled as water motion changes with time. To cancel the bedforms that are not in equilibrium with the new conditions, a certain mass of sand must be removed.

Figure 9. Typical bedforms on the physically stratified sands facies. A), B), C) and D) are ordered from upstream to downstream. Rip-up-clasts are predominantly observed downstream in areas with symmetrical sandwaves (e.g. D). For location see Figure 6A.

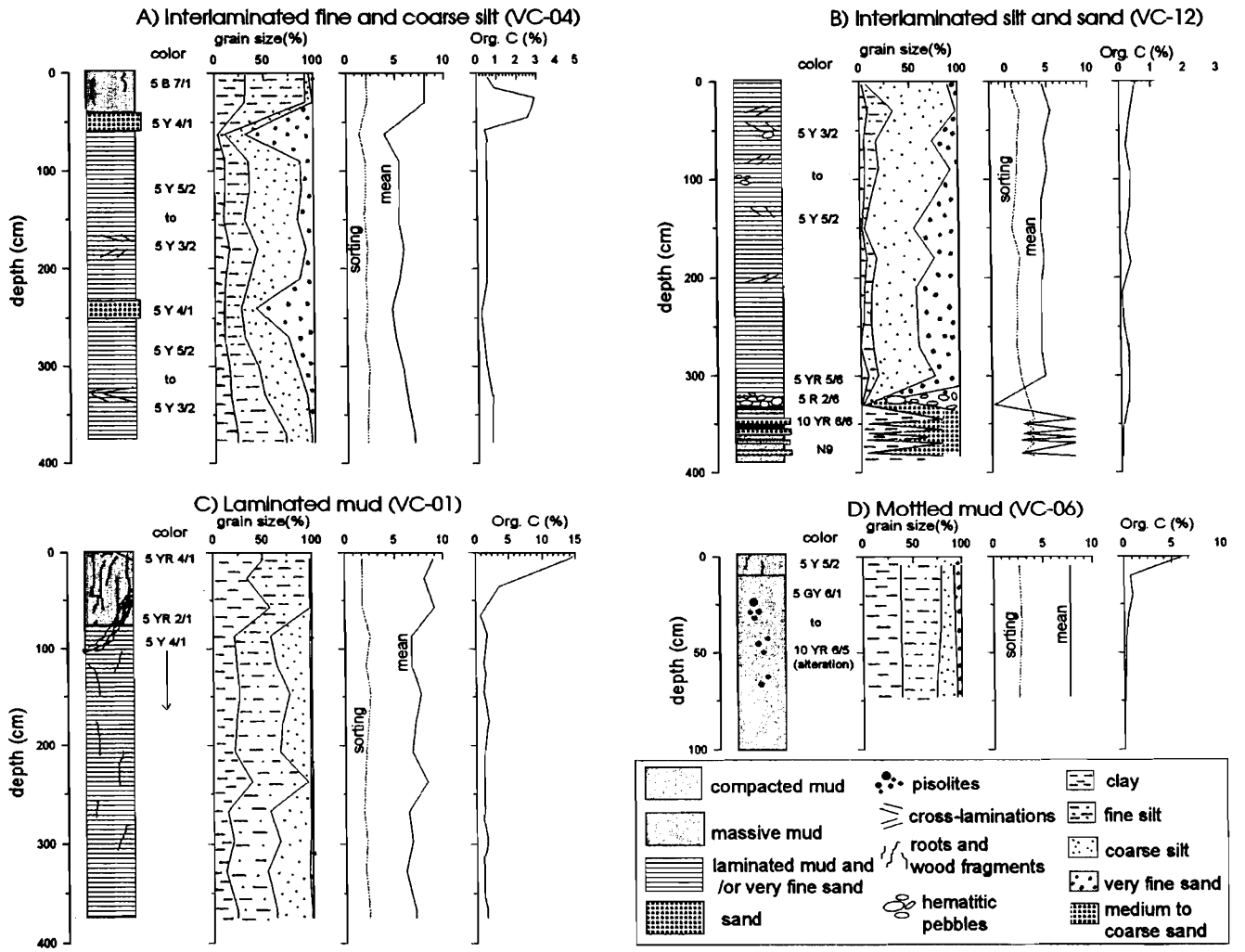

Figure 10. Typical core profiles showing the four sedimentary facies with vertical variation in color (Color code taken from Rock Color Chart), grain size, sorting, mean and organic-carbon content (Org. C.). For location see Figure 6A.

the faintly laminated mud facies is the absence of sand beds. This probably results from the position of the Estreitos area somewhat more distal relative to the source (Amazon), inducing a decreased supply of sand and coarse silt.

Mottled Mud. This facies is observed in cores taken from the interior of the islands, in places which are not normally reached by river water or which are exposed during low waters. It is characterized by massive compacted mud as well as by the presence of pisolites (concentric iron oxide and hydroxide, ranging from mm to cm). Wood fragments and roots are observed throughout. Invariably, the upper 5 cm consist of soft mud. Grain-size is similar to the faintly laminated mud facies. Mottled mud facies may represent soil development in a humid climate, where primary stratification was destroyed by root emplacement and bioturbation, giving the beds a mottled appearance.

Interlamination and interbedding of sand and mud at the river mouth result from the combination of fluvial and tidal processes. The grain-size variations may reflect temporal variations in flow; these regular changes can be of short duration (*e.g.* tidal changes) or they can be long-term changes (*e.g.* seasonal variations in Amazon sediment discharge). As demonstrated by JAEGER and NITTROUER (1995) on the Amazon Shelf near the river mouth, interlaminations can be produced semidiurnally due to tidal fluctuations, as well as fortnightly during periods of moderate tidal energy; interbedding there is entirely a fortnightly feature.

SUMMARY AND CONCLUSIONS

Suspended sediment concentration measurements show that net deposition occurs on the delta plain (between Obidos and the Xingu River), while downstream suspended sediment transport remains approximately constant. Lateral sediment input is compensated by erosion in deeply incised channels keeping this region in a dynamic equilibrium.

The mapped surficial distribution of sediments carried by the Amazon shows a corridor of sands (channel deposits) bordered by silty sediments at the margins. It consists chiefly of very fine sands that change laterally to fine and medium-coarse sands, designated physically stratified sands. The development of bedforms on the sand surface reflects strong bottom currents and sediment transport as well as tidal effects. Sedimentary facies identified in the sediment of the Amazon margins are interlaminated fine and coarse silt, interlaminated silt and sand, Faintly laminated mud, and mottled mud.

In this study intense erosion was observed in the lowermost Amazon evidenced by steeply incised channels. This erosional activity may be triggered by tectonic uplift as postulated by DRISCOLL and KARNER (1994) who interpret the Gurupa arch as an active forebulge resulting from lithospheric flexure due to the high sediment load of the submarine Amazon fan-system.

The overconsolidated substrates near Macapa and Afua clearly delineated different hydraulic conditions in an old river bed. The substrate near Macapa was related to the Barreiras Formation, while another one near Afua could be related to the lake stage postulated by IRION *et al.* (1995). According to these authors, the maximum extent of the lake was reached when the velocity of sea-level rise decreased around 6000 years BP. Recent AMS-dating from the corresponding substrate in the North Channel (Caviana de Dentro island) gives an age of 12020 ± 80 ^{14}C years BP (TORRES, 1997). This reflects inundation and incision caused by the post-Pleistocene sea-level rise.

The complexity of the area arises from the interplay between the high energy river system and the marine energy spectrum driven by wind-generated waves and tides. This interplay results in patterns of erosion and deposition controlled by interactions of fluvial and oceanic processes.

ACKNOWLEDGMENTS

This work was part of a Ph.D. thesis from the first author supported by the Brazilian National Research Council (CNPq) and by the German Research Agencies DFG, GTZ. We are thankful to the help of L.E.C. Faria Jr. and colleagues from the "Programa the Pesquisa e Ensino em Ciencias do Mar-PROMAR" during field work. Many thanks are also to the pilots, Artemio and Tuica, of the Research Boat "CURUPIRA". We are gratefully to G. Kineke (University of South Carolina), Richard Limeburner and J. Candela (WHOI) for assistance in field with oceanographic equipment. The Para University (UFPa)-Brazil provided space, the infrastructure and the boat for field work. All analyses were carried on laboratories from the Kiel University.

LITERATURE CITED

BEARDSLEY, R.C.; CANDELA, J.; LIMEBURNER, R.; GEYER, W.R.; LENTZ, S.J.; CASTRO, B.M.; CACCHIONE, D., and CARNEIRO, N., 1995. The M_2 tide on the Amazon shelf. *Journal of Geophysical Research,* 100, 2283–2319.

CURTIS, W.F.; MEADE, R.H.; NORDIN JR., C.F.; PRICE, N.B., and SHOLKOVITZ, E.R., 1979. Non-uniform vertical distribution of fine sediment in the Amazon River. *Nature,* 280, 381–383.

DHN BRAZILIAN AGENCY, 1981. *Cartas de correntes rio Amazonas. Da barra norte ao porto de Santana.* DHN, 16p.

DRISCOLL, N.W., and KARNER, G.D., 1994. Flexural deformation due to Amazon Fan loading: a feedback mechanism affecting sediment delivery to margins. *Geology,* 22, 1015–1018.

FRANZINELLI, E., and POTTER, P.E., 1983. Petrology, chemistry, and texture of modern river sands, Amazon River System. *Journal of Geology,* 91, 23–39.

GIBBS, R.J., 1967. The geochemistry of the Amazon River system: part 1. The factors that control the salinity and the composition and concentration of the suspended solids. *Geological Society of America Bulletim,* 78, 1203–1232.

IRION, G.; MULLER, J.; MELLO, J.N., and JUNK, W.J., 1995. Quaternary geology of the Amazonian Lowland. *Geo-Marine Letters,* 15, 172–178.

IRION, G., and ZÖLLMER, V., 1990. Pathways of fine-grained clastic sediments—Examples from the Amazon, the Weser Estuary, and the North Sea. *In:* HELING, D.; ROTHE, P.; FÖRSTNER, U., and STOFFERS, P. (eds.), *Sediments and Environmental Geochemistry, Selected Aspects and Case Histories.* Spring-Verlag, pp. 351–366.

JAEGER, J.M., and NITTROUER, C.A., 1995. Tidal controls on the formation of fine-scale sedimentary strata near the Amazon river mouth. *In:* NITTROUER, C.A., and KUEHL, S.A. (eds). *Geological Significance of Sediment Transport and Accumulation on the Amazon Continental Shelf. Marine Geology,* 125, 259–281.

KUEHL, S.A.; NITTROUER, C.A., and DEMASTER, D.J., 1986. Distribution of sedimentary structures in the Amazon subaqueous delta. *Continental Shelf Research,* 6, 311–336.

KUEHL, S.A.; NITTROUER, C.A., and DEMASTER, D.J., 1988. Microfabric study of fine-grained sediments: observations from the Amazon subaqueous delta. *Journal of Sedimentary Petrology,* 58, 12–23.

KUEHL, S.A.; LEVY, B.M.; MOORE, W.S., and ALLISON, M.A., 1997. Subaqueous delta of the Ganges-Brahmaputra river system. *Marine Geology,* 144, 81–96.

MEADE, R.H., 1988. Movement and storage of sediment in river systems. *In:* LERMAN and MEYBECK (eds). *Physical and Chemical Weathering in Geochemical Cycles.* pp. 165–179.

MEADE, R.H., 1994. Suspended sediments of the modern Amazon and Orinoco Rivers. *Quaternary International,* 21, 29–39.

MEADE, R.H.; DUNNE, T.; RICHEY, J.E.; SANTOS, U.M., and SALATI, E., 1985. Storage and remobilization of suspended sediment in the lower Amazon river of Brazil. *Science,* 228, 488–490.

MEADE, R.H.; RAYOL, J.M.; DA CONCEIÇÃO, S.C., and NATIVIDADE, J.R.G., 1991. Backwater effects in the Amazon River Basin of Brazil. *Environmental Geology,* 18, 105–114.

MILLIMAN, J.D.; SUMMERHAYES, C.P., and BARRETO, H.T., 1975. Quaternary sedimentation on the Amazon continental margin: a model. *Geological Society of America Bulletim,* 86, 610–614.

NITTROUER, C.A., and DEMASTER, D.J., 1996. Oceanography of the Amazon Continental Shelf. *Continental Shelf Research,* 16, 5/6.

NITTROUER, C.A., and KUEHL, S.A., 1995. Geological Significance of Sediment Transport and Accumulation on the Amazon Continental Shelf. *Marine Geology,* 125, 3/4.

NITTROUER, C.A.; KUEHL, S.A.; STERNBERG, R.W.; FIGUEIREDO JR, A.G., and FARIA JR, L.E.C., 1995. An introduction to the geological significance of sediment transport and accumulation on the Amazon continental shelf. *In:* NITTROUER, C.A., and KUEHL, S.A. (eds). *Geological Significance of Sediment Transport and Accumulation on the Amazon Continental Shelf. Marine Geology,* 125, 177–192.

NORDIN, C.F.; MEADE, R.H.; CURTIS, W.F.; BOSIO, N.J., and LANDIM, P.M.B., 1980. Size distribution of Amazon River bed sediment. *Nature,* 286, 52–53.

OLTMAN, R.E., 1968. Reconnaissance investigations of the discharge and water quality of the Amazon River. *U.S. Geological Survey Circular,* 552, 16p.

REID, I., and FROSTICK, L.E., 1994. Fluvial sediment transport and deposition. *In:* PYE, K. (ed). *Sediment Transport and Depositional Processes.* New York: Blackwell, pp. 89–155.

RICCI-LUCCHI, F., 1995. *Sedimentographica-Photographic Atlas of Sedimentary Structures.* Columbia University Press, 255p.

TANNER, W.F., 1991. Suite statistics: The hydrodinamic evolution of the sediment pool. *In:* SYVITSKI, J.P.M. (ed). *Principles, Methods and Application of Particle Size Analysis.* Cambridge: Cambridge university Press, pp. 225–236.

TANNER, W.F., 1995. William f. Tanner on Environmental Clastic Granulometry. *Florida Geological Survey Special Publication n. 40,* 142p.

TORRES, A.M., 1997. Sedimentology of the Amazon Mouth: North and South Channels, Brazil. Ph.D. thesis. Kiel University. Germany. 145p.

TORRES, A.M. and STATTEGGER, K., 1995. Bottom sediment distribution and suspended sediment concentration in the Amazon River mouth region: North and South Channels. *V Congresso da Associacao Brasileira de Estudos do Quaternario*/XI Simposio de sedimentologia costeira. ANAIS, UFF-Niteroi, RJ. pp. 114–119.

TRASK, P.D., 1939. Organic content of Recent marine sediments in recent marine sediments. (TRASK, ed). *American Association of Petroleum Geologist,* Tulsa, pp. 428–453.

TYSON, R.V., 1995. *Sedimentary Organic-Matter Facies and Palynofacies.* New York: Chapman & Hall, 615p.

VITAL, H., 1996. Sedimentology of the Lowermost Amazon (Rio Xingu–Macapa) and the "*Estreitos de Breves*"—*Brazil.* Ph.D. thesis. Kiel University. Germany. 189p.

VITAL, H.; STATTEGGER, K.; POSEWANG, J., and THEILEN, F., 1998. Lowermost Amazon River: morphology and shallow seismic characteristics. *Marine Geology,* 152, 277–294.

VITAL, H.; STATTEGGER, K., and GARBE-SCHÖNBER, D-C, 1999. Mineralogy and geochemistry (REE and trace elements) of clays and heavy minerals of the lowermost Amazon River: A provenance study. *Journal of Sedimentary Research*, 69, 563–575.